Analysis of necking in cylindrical bar of hardening materials

L. DIETRICH (WARSZAWA)

THE PROBLEM of necking in an axisymmetric tension specimen made of a strain-hardening material is investigated by means of a numerical procedure. The developed condition of necking depends on the hardening rate of a material and length to the diameter ratio of a specimen. The results of the experiments are in good agreement with the theoretical predictions.

W pracy przedstawiono numeryczną analizę procesu tworzenia się szyjki w rozciąganej, osiowo-symetrycznej próbce wykonanej z materiału ze wzmocnieniem. W otrzymanym warunku powstanie szyjki zależy od modułu umocnienia materiału i stosunku długości do średnicy próbki. Przeprowadzone doświadczenia potwierdzają wyniki teoretyczne.

В работе представлен численный анализ процесса образования горловины в растягиваемом, осесимметричном образце, изготовленном из материала с упрочнением. В полученном условии возникновение горловины зависит от модуля упрочнения материала и от отношения длины к диаметру образца. Проведенные эксперименты подтверждают теоретические результаты.

1. Introduction

THIS PAPER deals with the phenomenon of necking in a circular cylindrical bar pulled in tension. The condition of neck formation and the influence of the hardening rate and dimensions of a specimen on the onset of necking is considered.

The range of uniform strain under uniaxial tension can be under some circumstances much greater than the value of strain at which load reaches maximum. In 1955 KELLER [1] (see also [2]) observed that for a specimen made of zirconium and subject to tensile stresses at elevated temperature (200–370°C), the necking initiated at the strain ten times greater than the strain at maximum load. A similar effect was also observed for specimen made of zinc and tensile at room temperature [3].

General conditions of necking for an elastic-plastic material with hardening were considered by MILES [4], CHENG, ARIARATNAM and DUBEY [5] making use of the mathematical theory of bifurcation. They established that the onset of necking depends on the dimensions of a bar. Bifurcation occurs nearer to the maximum-load point for slender bars than for stubby ones.

Also the results of numerical analysis [6, 7] showed that necking appears beyond the maximum-load point and that the onset of necking is affected by the initial length to the diameter ratio. CHEN [6] used a generalized plastic flow theory for large deformation and assumed an imperfection to initiate necking. For a given power of the hardening law and initial length to the diameter ratio of a specimen equal to 2 stresses and deformations were calculated by a step-by-step method. Unloading, which appeared at some instant at the ends of the bar, was treated as the onset of necking.

The finite element method was used in the analysis of necking by NEEDLEMAN [7]. The onset of necking was determined as a bifurcation from a state of uniform tensile stress based on Hill's theory of bifurcation. Assuming a power hardening law, numerical calculations were performed for two values of initial length to the diameter ratio (equal to 4 and 2) and two different types of end conditions (cemented ends to rigid grips and shear stress free ends).

The effect of specimen dimensions on the onset of necking was also pointed out in the analysis of necking of tensile specimen under plane strain conditions by COWPER and ONAT [8] as well in the analysis of stability of an elastic cylinder under uniaxial stress by WESOŁOWSKI [9].

In this paper the instant at which necking occurs is determined from a comparison of increments of load for the uniform deformation mode and the localized, in a central region of the specimen, deformation mode. The load for the localized deformation mode as a function of the hardening rate of a material and the ratio of length to the diameter of the specimen is calculated by means of a numerical procedure in which the plastic flow problem for the hardening material is formulated as a succession of incremental problems.

2. Basic equations

The method of solving axially-symmetric plastic flow problems with hardening of a material taken into account which will be used in this analysis of necking was described in details in [10]. In this section only the basic equation and method of the numerical calculations used in the analysis are presented.

For the axially-symmetric case we have two equations of equilibrium

$$(2.1) \qquad \frac{\partial \sigma_r}{\partial r} + \frac{\partial \tau_{rz}}{\partial z} + \frac{\sigma_r - \sigma_\theta}{r} = 0,$$

$$\frac{\partial \tau_{rz}}{\partial r} + \frac{\partial \sigma_z}{\partial z} + \frac{\tau_{rz}}{r} = 0.$$

The Tresca yield condition for materials with isotropic hardening takes the form

$$(2.2) \qquad (\sigma_r - \sigma_z)^2 + 4\tau_{rz}^2 = 4k^2,$$

where the yield point in shear is dependent on the path of plastic strains ε_i defined as

$$(2.3) \qquad \varepsilon_i = \sqrt{\frac{2}{3}} \int\limits_0^{\varepsilon_{ij}^p} \sqrt{d\varepsilon_{ij}^p d\varepsilon_{ij}^p}.$$

If we assumed the Haar-Kármán criterion in the form

$$(2.4) \qquad \sigma_2 = \sigma_3 = \sigma_\theta,$$

the set of equations for stresses becomes statically determinate (i.e. the equations for stresses may be solved independently of the velocity equations) under the condition that the distribution of the yield point in shear $k(r, z)$ is known over the plastic region.

One can point out that the set of equations (2.1), (2.2), (2.4) is hyperbolic [11, 12] and can be solved by means of the characteristics method. The equations of the characteristics are

(2.5)
$$\frac{dz}{dr} = \tan(\varphi - 45°) \quad \text{called as} \quad \alpha,$$

$$\frac{dz}{dr} = \tan(\varphi + 45°) \quad \text{called as} \quad \beta,$$

where φ is the angle between the σ_1 and r-directions. For a varying yield-stress k, the relationships along the characteristics' directions are

(2.6)
$$dp - 2kd\varphi = \frac{\partial k}{\partial r} dz - \frac{\partial k}{\partial z} dr + \frac{k}{r}(dz - dr) \quad \text{along } \alpha\text{-lines},$$

$$dp + 2kd\varphi = \frac{\partial k}{\partial z} dr - \frac{\partial k}{\partial r} dz - \frac{k}{r}(dz + dr) \quad \text{along } \beta\text{-lines},$$

where $p = 0.5 (\sigma_1 + \sigma_2)$.

The velocity components v_r, v_z along the r and z-directions are determined by the incompressibility condition

(2.7)
$$\frac{\partial v_r}{\partial r} + \frac{\partial v_z}{\partial z} = -\frac{v_r}{r},$$

and the isotropy condition

(2.8)
$$\frac{\partial v_r}{\partial z} + \frac{\partial v_z}{\partial r} - \left(\frac{\partial v_r}{\partial r} - \frac{\partial v_z}{\partial z} \right) \tan 2\varphi = 0.$$

The system of Eqs. (2.7) and (2.8) is also hyperbolic. The relationships along the characteristics' lines are the same as for a homogeneous, perfectly-plastic material [13]:

(2.9)
$$dv_r + dv_z \tan(\varphi - 45°) = \frac{v_r}{r} \frac{dz}{\cos 2\varphi} \quad \text{along } \alpha\text{-lines},$$

$$dv_r + dv_z \tan(\varphi + 45°) = -\frac{v_r}{r} \frac{dz}{\cos 2\varphi} \quad \text{along } \beta\text{-lines}.$$

3. Numerical method

In the present paper the numerical procedure for the axially-symmetric necking problem, with hardening of a material taken into account, consists in dividing the deformation process into a number of stages. In each of the stages we calculate:

stresses from Eqs. (2.5) and (2.6),

flow velocities from Eqs. (2.9),

components of the strain rate tensor by means of numerical differentiation of the flow velocity components,

displacement for each particle of the plastic zone assuming that in a sufficiently small time increment the flow velocities are constant,

the value of the hardening parameter from Eq. (2.3) for each particle of the plastic zone,

the distribution of the yield point non-homogeneity based on the assumed stress-strain relationship of a material.

In this procedure the problem of plastic flow at the instant when necking appears under the tension of an axially-symmetric rod made of a hardening material is formulated as a succession of incremental problems for a perfectly plastic, non-homogeneous material. On the basis of a comparison of loads for two stages of deformation, we are able to calculate the increment of load which produces a definite elongation of the bar for the local deformation mode. As a starting point the velocity field proposed by EASON and
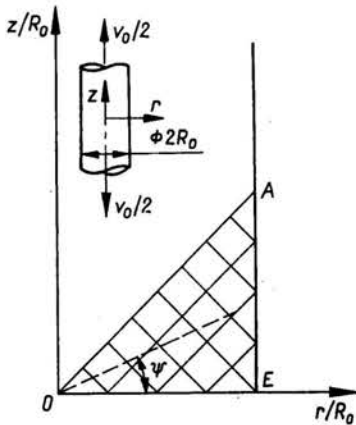

FIG. 1. The slip-line field for circilar cylinder pulled in tension.

SHIELD [14] has been assumed. The plastic flow is confined to the material below AO (Fig. 1) and the velocity components in r and z-directions are given in the form

(3.1)

$$v_r = -\frac{v_0}{\pi}\sqrt{1-\tan^2\psi},$$

$$v_z = v_0\left[0.5 - \frac{1}{\pi}\arccos(\tan\psi)\right],$$

where ψ denotes the inclination of the radius vector of a particular point to the r-axis and v_0 denotes the relative velocity of the rigid parts of the bar.

In the first stage of calculations the rod is under uniaxial and uniform stress state. The velocity field is given by Eq. (3.1). The components of the strain rate tensor are given by

(3.2)

$$\dot{\varepsilon}_r = -\frac{v_0}{\pi r}\frac{\tan^2\psi}{\sqrt{1-\tan^2\psi}},$$

$$\dot{\varepsilon}_z = \frac{v_0}{\pi r}\frac{1}{\sqrt{1-\tan^2\psi}},$$

$$\dot{\varepsilon}_\theta = -\frac{v_0}{\pi r}\sqrt{1-\tan^2\psi},$$

$$\dot{\varepsilon}_{rz} = 0.$$

Further steps of calculations take a course according to the numerical procedure described above. The calculated distribution of the yield point non-homogeneity and the shape of the free surface AE (Fig. 2) constitutes the boundary conditions of a second stage of calculations. Basing on the slip-line solution of the stage shown in Fig. 2, one can
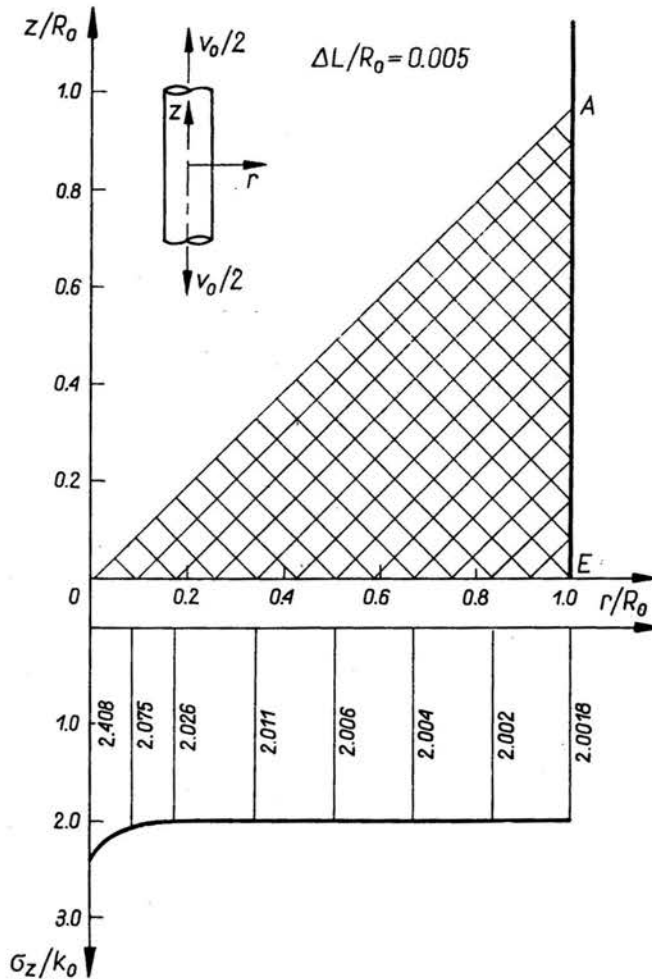

FIG. 2. The slip-line field and distribution of the axial stresses at the neck for second stage of calculations.

calculate the total axial load P^* by means of numerical integration of the axial stress acting at the minimum cross-section of the neck. The total elongation ΔL of a rod is defined by the velocity field and the assumed value of the time increment between stages. From a comparison of loads in the first and second stage of calculations, one can determine, for the local deformation mode, the increment of load ΔP^* which produces a definite value of a total elongation ΔL of a rod. Since we are interested in the value of ΔP^* at the instant when necking begins, our calculations are limited to the first and second stage. The value of ΔP^* is calculated under the assumption of a linear stress-strain relationship

of a material beyond the range of uniform strain (Fig. 3). The form of the stress-strain curve ·in a range of smaller strains can be arbitrary. States of stresses and strains are uniform up to the onset of necking (point B, Fig. 3). The assumption of a hardening law
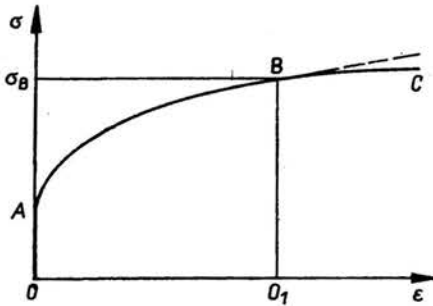

FIG. 3. Schematic diagram of the stress-strain curve.

in a linear form enables us to represent the load increment ΔP^* for the local deformation mode as a function of the hardening rate defined by the relationship

$$(3.3) \qquad\qquad h = \frac{1}{\sigma} \cdot \frac{d\sigma}{d\varepsilon}.$$

A linear stress-strain relationship at the end of the uniform strain range is frequently observed for real materials. On the other hand the approximation of a real characteristic of a material by the tangent line has small influence on the value of the load increment calculated for very small elongation of a rod.

4. Results of numerical calculations

Numerical calculations of the load increment for the local deformation mode of an axially-symmetric rod pulled in tension have been performed according to the procedure described above assuming the stress-strain relationship of a material in the linear form:

$$(4.1) \qquad\qquad k/k_B = 1 + h \cdot \varepsilon_i,$$

where k_B denotes the value of the yield point in shear of a material at the instant of the onset of necking (see Fig. 3), ε_i is the hardening parameter defined by Eq. (2.3), h is the hardening rate defined by Eq. (3.3).

For different values of h in the range of 0 to 5 the load P^* in the second stage of deformation was calculated assuming different values of the total elongation ΔL of a rod. The results of those calculations in the case of $h = 2$ are shown by open circles in Fig. 4. In the considered range of the value h the dimensionless load P^*/P_B has a linear course with respect to the dimensionless total elongation $\Delta L/R_B$, where $2R_B$ and $P_B = 2k_B \cdot \pi R_B^2$ denotes the diameter of a rod and the load at the onset of necking respectively. On the basis of those calculations the ratio of ΔP^* over $\Delta L/R_B$ as a function of h has been determined. The results are shown in Fig. 5 in the range of $h = 0$ to 5 and in Fig. 6 for a narrow range up to the value of h equal to 1. The results of calculations obtained by
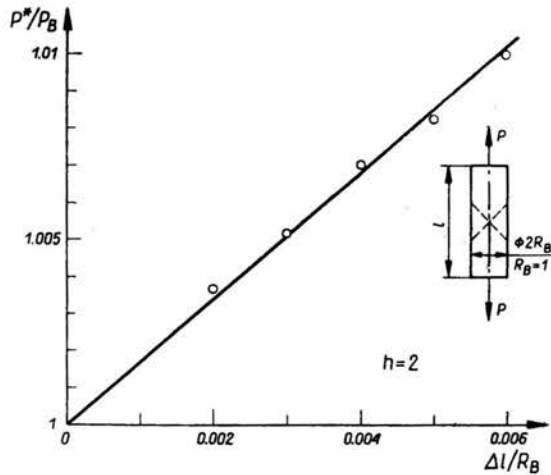
FIG. 4. The ratio of loads at the second and first stages of calculation as a function of the elongation increment between stages.
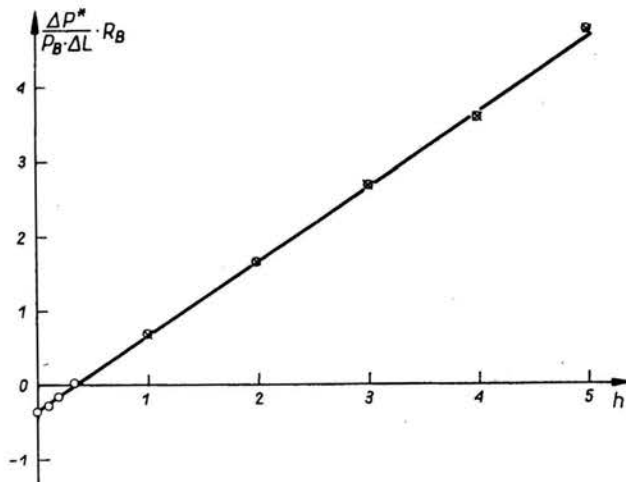

FIG. 5. The ratio of dimensionless increment of load to the dimensionless elongation versus the hardening rate h for the local deformation mode.

means of two numerical algorithms are shown by open circles and crosses. In each of these algorithms the method of interpolation of the ε_i value at nodal points was different. The calculated points are located along the straight line which intersects the h-axis at the value of $h = 0.35$. The scatter which is seen in Fig. 6 results from the numerical technique of computations.

Basing on these results, the increment of load for the local deformation mode can be expressed in such a simple form:

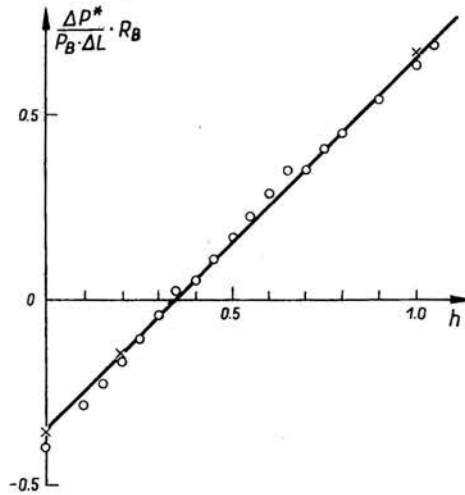$$(4.2) \qquad (dP^*)_B = \frac{P_B}{R_B}(h-0.35)dL.$$

5*

FIG. 6. The relationship from Fig. 5 for small values of h. Calculated points are shown by circles and crosses.

It is worth stressing that the relationship (4.2) was found without specification of the stress-strain curve of a material over the uniform strain range. The increment of load dP^* for the local deformation mode depends on the value of the hardening parameter h of a material at the instant when necking begins.

5. Condition of necking

We assume that necking begins at the instant when the increment of load dP^* for the local deformation mode which produces a definite elongation ΔL of a rod is not greater than the increment of load dP for the uniform deformation mode which gives the same value of the elongation of a rod. It can be written as

$$(5.1) \qquad \frac{dP^*}{dL} \leqslant \frac{dP}{dL}.$$

The increment of load dP for the uniform deformation mode can be easily calculated assuming that the stress-strain curve of a material is known.

Let us assume that the stress-strain relationship is given by

$$(5.2) \qquad \sigma = C\varepsilon^n,$$

where C and n are material constants, σ is the true stress and ε the natural strain.

The axial tensile load defined as

$$(5.3) \qquad P = \sigma \cdot A,$$

where A denotes the current cross-sectional area of a rod, can be written in the form

$$(5.4) \qquad P = C[\ln(L/L_0)]^n A_0 \frac{L_0}{L}$$

assuming the constant volume condition. A_0 is the initial cross-sectional area and L_0 the initial length of a specimen. The increment of load dP for the uniform deformation mode can be found by means of the differentiation of Eq. (5.4) with respect to L and is given by

$$(5.5) \qquad (dP)_B = \frac{P_B}{L_B}(h-1)dL,$$

where for the assumed stress-strain relationship (5.2) the hardening rate is equal to

$$(5.6) \qquad h = \frac{n}{\varepsilon}.$$

On substituting Eqs. (4.2) and (5.5) into Eq. (5.1), the condition of necking for materials described by the power hardening law in the form (5.2) can be written as

$$(5.7) \qquad \frac{L_B}{R_B} \geqslant \frac{h-1}{h-0.35},$$

where $2R_B$ is the diameter and L_B the length of a rod at the onset of necking.
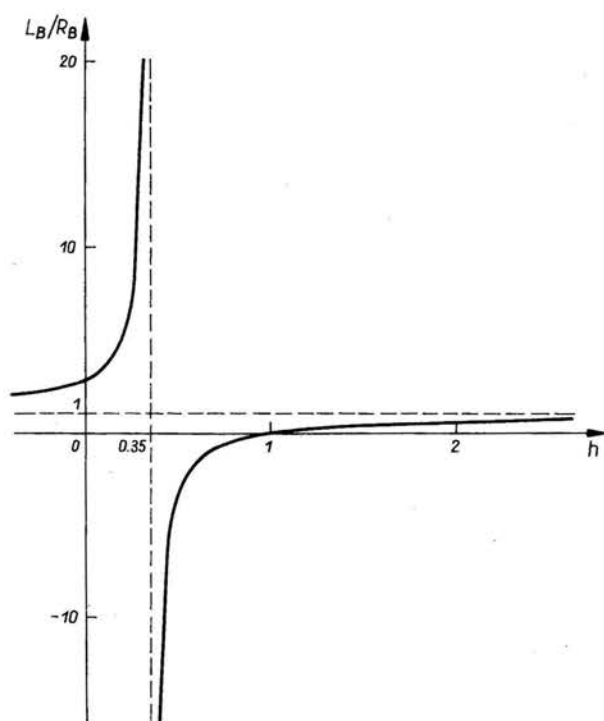

FIG. 7. The ratio of length to half the diameter of a specimen at the onset of necking as a function of the hardening rate of a material.

The L_B/R_B ratio as a function of the hardening parameter h is shown in Fig 7. The slip-line solution (Fig. 1) used in this analysis is valid for the $L_B/R_B \geqslant 2$, thus only the upper curve in Fig. 7 has a physical meaning.

Taking into consideration the definition of strain ($\varepsilon = \ln(L/L_0)$) and the relationship (5.6), one can express the value of strain ε_B at the onset of necking as a function of the initial dimensions L_0/R_0 ratio. The condition of necking (5.7) takes the form

(5.8)
$$\frac{L_0}{R_0} \geqslant \frac{n - \varepsilon_B}{n - 0.35\varepsilon_B} e^{-\frac{3}{2}\varepsilon_B}.$$
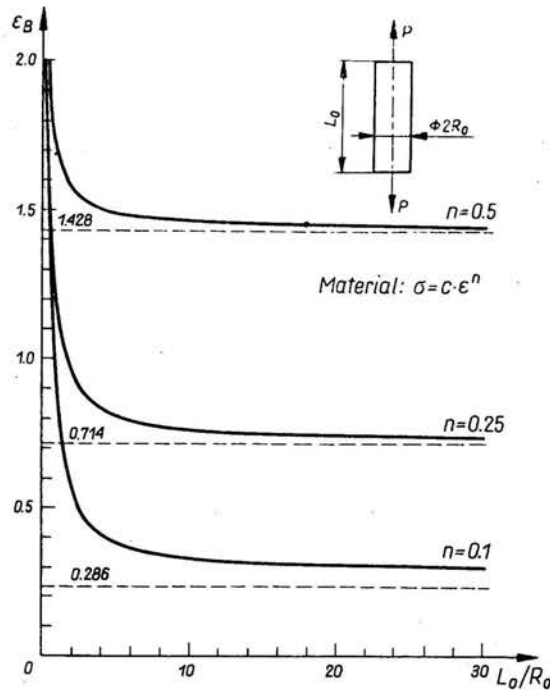

FIG. 8. The value of the maximum uniform strain versus the initial length to half the diameter ratio for different values of the exponent of the assumed power hardening law of a material.

Plots of $\varepsilon_B = f(L_0/R_0)$ are shown in Fig. 8 for different values of the hardening exponent n. The initial length to the diameter ratio has small influence on the value of strain ε_B for $L_0/R_0 > 10$. But even for infinitely long specimens, the values of ε_B shown in Fig. 8 by broken lines are much greater than the values of strain $\varepsilon_P = n$ at which load reaches the maximum.

Let us assume that specimens are made of two materials which can be described by the relationship (5.2) with the constant C equal to 500 MN/m² and the hardening exponent n equal to 0.25 and 0.5, respectively. The stress-strain relationships for both considered materials are shown in Fig. 9a. Plots of a tensile load referred to the initial cross-sectional area A_0 versus the natural strain are shown in Fig. 9b by a solid and broken line for $n = 0.25$ and $n = 0.5$ respectively. The curves were calculated assuming uniform deformation and a constant volume of the specimen. The load reaches the maximum value at the strain $\varepsilon = n$. The onset of necking calculated according to the condition (5.8) is shown by small circles for specimens with different initial length to the diameter ratio. The course of the
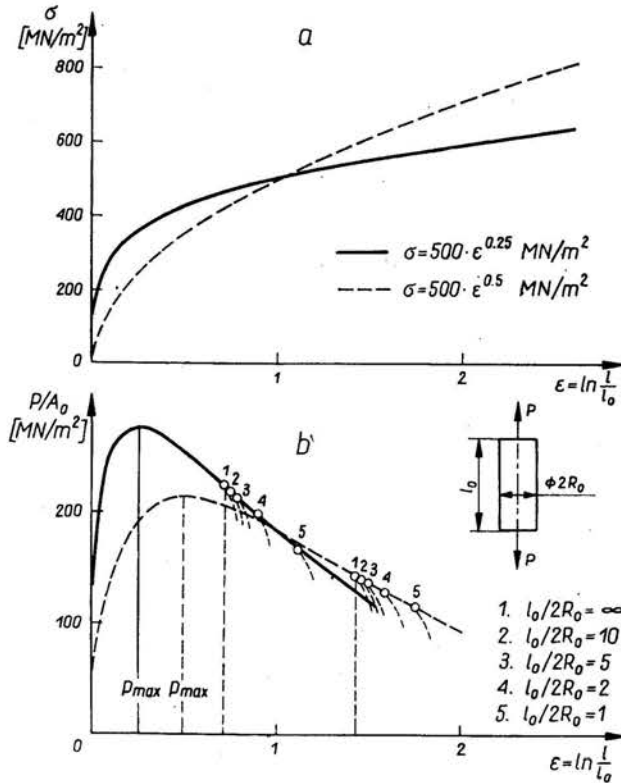
FIG. 9. The assumed two stress-strain curves (a) and calculated plots of the axial load versus strains for specimens with different values of the length to the diameter ratio (b).

load versus strain diagrams beyond the range of uniform strains is schematically shown by the fine broken lines. The onset of necking occurs nearer to the point of maximum load for longer rods than for shorter ones. The range of uniform strain is much greater than the value of strain at which load reaches maximum.

6. Results of experiments

In the case of real materials the stress-strain relationships are more complicated than the power hardening law in the form (5.2). In order to check if essential differences between strains at the maximum load and at the onset of necking shown in Fig. 9 will also be observed for real materials, tensile tests for specimens made of mild steel (denoted as 15 according to the Polish Standards) have been performed. The essential dimensions of the specimen are given in Fig..10. The specimen was pulled in tension with a constant crosshead speed equal to 0.5 mm/min using the INSTRON hydraulic testing maschine. The tensional load P, elongation Δl on the base of 10 mm and reduction of the specimen diameter $2\Delta r$ were measured during the test. The results for such a selected specimen in which necking occurred beyond the place where gauges were attached are shown as a func-
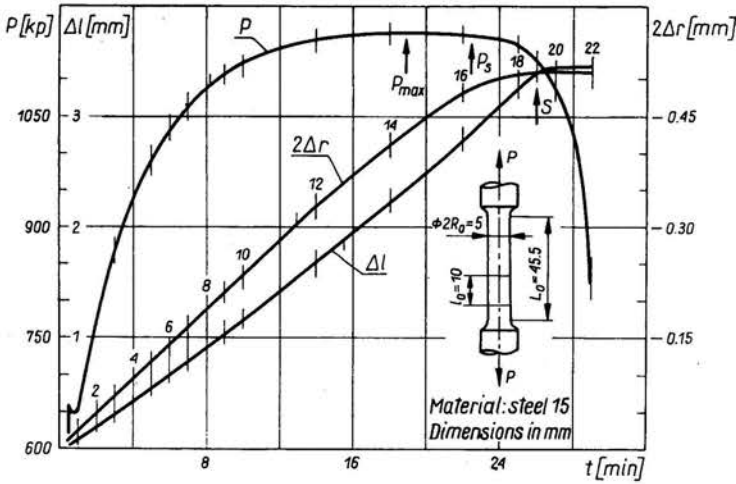
FIG. 10. Load, elongation and reduction of a diameter as a function of time during the tensile test of the specimen made of mild steel.

tion of time in Fig. 10. The identification points are shown by fine vertical lines. The arrow with the symbol P_{max} indicates the instant at which the load reaches the maximum value. At the instant marked by an arrow with the symbol S, strain localization can be observed as fogging of the initially polished surface of the specimen. The instant when necking occurs according to the criterion described is shown by an arrow with the symbol P_s. Since it was very difficult to find a sufficiently exact approximation of the real stress-strain curve in an analytical form, the dimensionless hardening rate and the increment of load for uniform deformation was found by means of graphical differentiation. Using the experimental results concerning the true stress-strain curve and the plot of the load versus the total elongation of the specimen can be determined in the following relationships:

$$f_1(\varepsilon) = \frac{1}{\sigma}\frac{d\sigma}{d\varepsilon},$$

(6.1)

$$f_2(\varepsilon) = \frac{1}{P}\frac{dP}{dL'},$$

where $L' = L/R_0$.

According to the inequality (5.1) and the relationship (4.2), the value of strain ε_B at the onset of necking is determined by the relationship

(6.2) $f_1(\varepsilon)-0.35 = e^{0.5\varepsilon}f_2(\varepsilon).$

In the considered example it was found that $\varepsilon_B = 0.25$ in comparison with the value of $\varepsilon_P = 0.21$ at which load reached the maximum. The ratio of $\varepsilon_B/\varepsilon_P$ is equal to 1.19.

It can be seen from Fig. 10 that the course of both $\Delta l = f(t)$ and $\Delta r = f(t)$ plots changes its character beyond the point 16. It is in agreement with the theoretical prediction.

The true stress — the natural strain curve — is plotted in Fig. 11 in the logarithmic scale. The change of the course of that curve also indicated that the onset of necking takes place beyond the point 16.
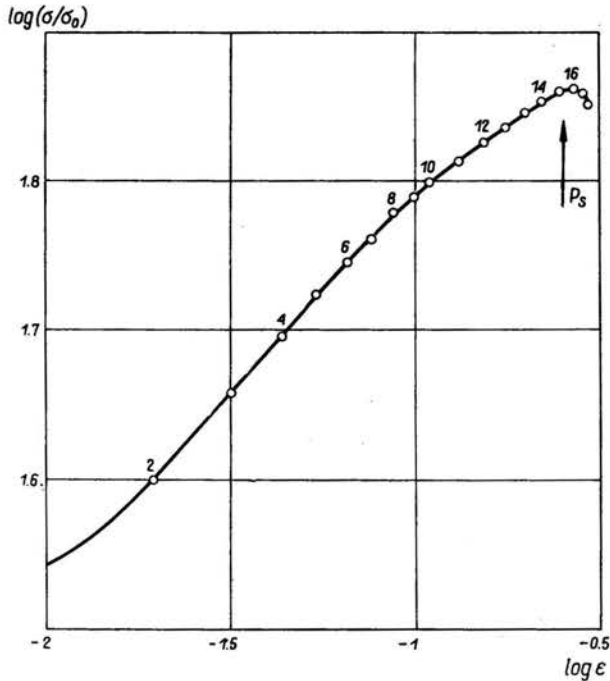
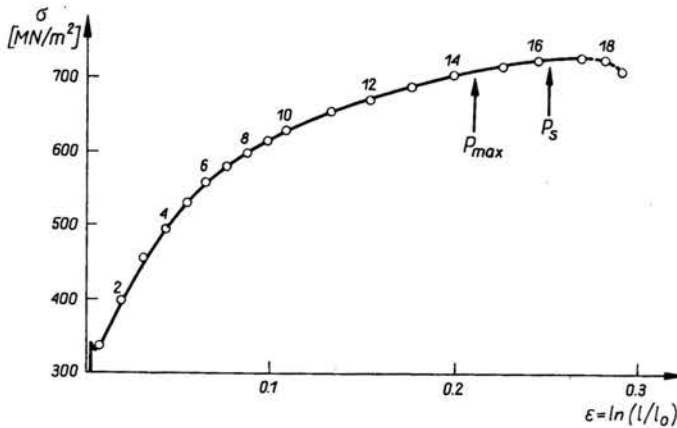FIG. 11. The stress-strain curve in the logarithmic scale for mild steel.

FIG. 12. The true stress- the natural strain curve for mild steel. Arrows indicate the maximum load point and the onset of necking.

The plot of true stresses as a function of natural strains in the plastic range is shown in Fig. 12. The range of uniform deformation in the simple tension test of the considered mild steel is about 20% greater than the value of strain at the maximum load point.

7. Concluding remarks

The strain at the onset of necking is found on the basis of a comparison of increments of loads for the uniform and local deformation modes. Calculations of the load increment in the case of local deformation have been based on the assumed flow velocity field. It follows that the strain at the onset of necking is greater than that at the maximum load point and depends on the hardening rate of a material and the length to the diameter ratio of a specimen. The results of experiments performed on specimens made of mild steel are in good agreement with the theoretical predictions.

Considering present analysis, the onset of necking in a tension test can be easily determined from known relationships of both the hardening rate versus strains and load versus elongation of a specimen.

It is generally accepted that the onset of necking is influenced by two phenomena which are the hardening of a material and the decreasing of the cross-sectional area of a specimen. The results of this paper show that the geometrical changes associated with necking, which cause strengthening of the specimen at the minimum cross-section, have also an essential influence on the onset of necking.

References

1. J. H. Keeler, *The tensile characteristics of unalloyed zirconium at low and moderate temperatures*, Trans. Am. Soc. Metals, **47**, 157–192, 1955.
2. G. E. Dieter, *Mechanical metallurgy*, McGraw-Hill, 1961.
3. S. Katarzyński, S. Kocańda, M. Zakrzewski, *Investigation of the mechanical properties of metals* [in Polish], WNT, Warsaw 1967.
4. J. P. Miles, *Bifurcation in plastic flow under uniaxial tension*, J. Mech. Phys. Solids, **19**, 2, 1971.
5. S. Y. Cheng, S. T. Ariaratnam, R. N. Dubey, *Axisymmetric bifurcation in an elastic-plastic cylinder under axial load and lateral hydrostatic pressure*, Quart. Appl. Math., **29**, 1, 1971.
6. W. H. Chen, *Necking of a bar*, Int. J. Solids Structures, **7**, 7, 1971.
7. A. Needleman, *A numerical study of necking in circular cylindrical bars*, J. Mech. Phys. Solids, **20**, 2, 1972.
8. G. R. Cowper, E. T. Onat, *The initiation of necking and buckling in plane plastic flow*, Proc. 4th U.S. Nat. Congr. Appl. Mechs., ASME, **2**, 1023–1029, New York 1962.
9. Z. Wesołowski, *The axially-symmetric problem of stability loss of an elastic bar subject to tension*, Arch. Mech., **15**, 3, 383–395, 1963.
10. L. Dietrich, *Solving of the plastic flow problems for hardening materials* [to be published].
11. M. L. Devenpeck, A. S. Weinstein, *Experimental investigation of work-hardening effects in wedge flattening with relation to nonhardening theory*, J. Mech. Phys. Solids, **18**, 3, 1970.
12. H. G. Hopkins, *Mathematical methods in plasticity theory*, Problems of plasticity, A. Sawczuk (ed.), Noordhoff Int. Pub., 235–260, Leyden 1974.
13. R. T. Shield, *On the plastic flow of metals under conditions of axial symmetry*, Proc. Roy. Society, A, **233**, 267–286, 1955.
14. G. Eason, R. T. Shield, *The plastic indentation of a semi-infinite solid by a perfectly rough circular punch*, ZAMP, **11**, 1, 33–42, 1960.